

Hierarchical Equations of Motion Approach to Quantum Thermodynamics

Akihito Kato^{1,*} and Yoshitaka Tanimura^{2,†}

¹*Institute for Molecular Science, National Institutes of Natural Sciences, Okazaki 444-8585, Japan*

²*Department of Chemistry, Graduate School of Science,
Kyoto University, Sakyo-ku, Kyoto 606-8502, Japan*

(Dated: May 20, 2018)

We present a theoretical framework to investigate quantum thermodynamic processes under non-Markovian system-bath interactions on the basis of the hierarchical equations of motion (HEOM) approach, which is convenient to carry out numerically “exact” calculations. This formalism is valuable because it can be used to treat not only strong system-bath coupling but also system-bath correlation or entanglement, which will be essential to characterize the heat transport between the system and quantum heat baths. Using this formalism, we demonstrated an importance of the thermodynamic effect from the bath-system-bath tri-partite correlations (TPC) for a two-level heat transfer model and a three-level autonomous heat engine model under the conditions that the conventional quantum master equation approaches are failed. Our numerical calculations show that TPC contributions, which distinguish the heat current from the energy current, have to be taken into account to satisfy the thermodynamic laws.

INTRODUCTION

Recent progress in manipulating small-scale systems provides the possibility of examining the foundation of statistical mechanics in nano materials [1–3]. In particular, elucidating how such purely quantum mechanical phenomena as quantum entanglement and coherence are manifested in thermodynamics is of particular interest in the field of quantum thermodynamics [4, 5]. Such problems have been studied with approaches developed through application of open quantum dynamics theory.

Widely used approaches employ a quantum master equation (QME) that can be derived from the quantum Liouville equation with a system plus bath Hamiltonian by tracing out the heat bath degrees of freedom. To obtain time-evolution equations for the reduced density operator in a compact form, one usually employs the Markov approximation, in which the bath correlation time is very short in comparison to the characteristic time of the system dynamics. The QME with the second-order treatment of the system-bath interaction and the Redfield equation (RE) have been derived with the projection operator method, for example [6, 7]. As we will show in Fig. 1, however, even if the dissipation process is Markovian, the fluctuation process may not be, because the latter has to be related to the former through the fluctuation-dissipation theorem (FDT). For this reason, if we apply the QME under Markovian assumption to low temperature systems, then the positivity of the probability distributions of the reduced system cannot be maintained. As a method to preserve positivity, the rotating wave approximation (RWA), which eliminates the non-resonant interaction between the system and the heat bath, has been applied in order to write the master equation in the Lindblad form. However, this approximation may modify the thermal equilibrium state as well as the dynamics of the original total Hamiltonian, because the FDT is also altered. For example, while the true thermal equilibrium state of the system at inverse temperature β is given by $\text{Tr}_{\text{bath}}[\exp(-\beta\hat{H}_{\text{total}})]/\text{Tr}_{\text{total}}[\exp(-\beta\hat{H}_{\text{total}})]$, where \hat{H}_{total} and Z are the total system-plus-bath Hamiltonian, the thermal equilibrium state obtained from the second-order QME approach is $\exp(-\beta\hat{H}_{\text{sys}})/\text{Tr}_{\text{sys}}[\exp(-\beta\hat{H}_{\text{sys}})]$ where \hat{H}_{sys} is the bare system Hamiltonian. This implies that the Markovian assumption even in a perturbative system-bath coupling regime is incompatible through obtaining a quantum mechanical description of dissipative dynamics at low temperature[8]. Furthermore, the consistent description of the QME with the FDT is important to investigate the non-trivial quantum thermodynamic processes, because the violation of the FDT is responsible for the heat generation [9, 10].

As explained in the above, there is a strong limitation on the basis of the conventional QME approaches for the study of quantum thermodynamics, despite their successes to predict the performance of heat machines and propose systems. For example, the inconsistency between the global and local QME, in which the bath couples to the eigenstates of the system and the eigenstates of the sub-system, respectively, have to be reconciled even in a weak system-bath coupling regime [11, 12]. While the global QME can predict the Gibbs distribution in the equilibrium situations, some unphysical behavior caused by employing the global QME in the non-equilibrium situations are reported. Moreover, the local QME may violate the second law of thermodynamics. Attempt to recover the correct thermodynamic description of the global QME was made by incorporating the non-additive dissipation [13], which was not treated in the conventional QME approaches. The interplay between the quantum coherence and environmental

noise is essential to optimize the excitation energy and heat transport [14, 15] that should be clarified by using the non-perturbative and non-Markovian quantum dynamical theory [16].

To this time, the approaches used to study the strong coupling regime in the field of quantum thermodynamics include the QME employing a renormalized system-plus-bath Hamiltonian derived with the polaron transformation [17] or the reaction-coordinate mapping [18, 19], the non-equilibrium Green's function (NEGF) method [20–22], the functional integral approach [23], and the stochastic Liouville-von Neumann equation approach [24]. However, the QME with the renormalized Hamiltonians and the NEGF method are limited to a case with a slowly driving field. The stochastic Liouville-von Neumann equation approach is only applicable to the short-time region due to an enormous number of stochastic sampling.

Many of the above-mentioned limitations can be overcome with the hierarchical equations of motion (HEOM), which are derived by differentiating the reduced density matrix elements defined by path integrals [25–30]. This approach allows us to treat systems subject to external driving fields in a numerically rigorous manner under non-Markovian and non-perturbative system-bath coupling conditions and have been applied for the studies of quantum information theory [31, 32] and quantum thermodynamics [33, 34]. Moreover, non-additive dissipation can be incorporated into the HEOM approach through the explicit non-Markovian treatment of the reduced dynamics.

This Chapter presents the introduction of the HEOM for the open quantum dynamics and its application to the quantum thermodynamic processes by evaluating the heat current transferred between the system and the bath in a numerically rigorous manner. As we shown in ref. [34], the heat current is defined so as to be consistent with the first and second laws of thermodynamics by incorporating non-trivial tri-partite correlations. The exact reduced expression for the heat current and the way to numerically evaluate it through the use of the HEOM approach are presented. Then, the numerical illustrations of our approach are given for the two-level heat transfer model and the three-level autonomous heat engine model.

HIERARCHAL EQUATIONS OF MOTION APPROACH

We consider a system coupled to multiple heat baths at different temperatures. With K heat baths, the total Hamiltonian is written

$$\hat{H}(t) = \hat{H}_{\text{sys}}(t) + \sum_{k=1}^K \left(\hat{H}_{\text{int}}^{(k)} + \hat{H}_{\text{bath}}^{(k)} \right), \quad (1)$$

where $\hat{H}_{\text{sys}}(t)$ is the system Hamiltonian, whose explicit time dependence originates from the coupling with the external driving field. The Hamiltonian of the k th bath and the Hamiltonian representing the interaction between the system and the k th bath are given by $\hat{H}_{\text{bath}}^{(k)} = \sum_j \hbar \omega_{k,j} \hat{b}_{k,j}^\dagger \hat{b}_{k,j}$ and $\hat{H}_{\text{int}}^{(k)} = \hat{V}_k \sum_j g_{k,j} (\hat{b}_{k,j}^\dagger + \hat{b}_{k,j})$, respectively, where \hat{V}_k is the system operator that describes the coupling to the k th bath. Here, $\omega_{k,j}$, $g_{k,j}$, and $\hat{b}_{k,j}$ and $\hat{b}_{k,j}^\dagger$ are the frequency, coupling strength, and the annihilation and creation operators for the j th mode of the k th bath, respectively. We assume the factorized initial conditions, $\hat{\rho}_{\text{tot}}(0) = \hat{\rho}(0) \prod_{k=1}^K e^{-\beta_k \hat{H}_{\text{bath}}^{(k)}} / \text{Tr}(e^{-\beta_k \hat{H}_{\text{bath}}^{(k)}})$, where $\hat{\rho}$ is the reduced density operator of the system.

Due to the Bosonic nature of the bath, all bath effects on the system are determined by the bath correlation function, $C_k(t) \equiv \langle \hat{X}_k(t) \hat{X}_k(0) \rangle_{\text{B}}$, where $\hat{X}_k \equiv \sum_j g_{k,j} (\hat{b}_{k,j}^\dagger + \hat{b}_{k,j})$ is the collective coordinate of the k th bath and $\langle \dots \rangle_{\text{B}}$ represents the average taken with respect to the canonical density operator of the baths. The bath correlation function is expressed in terms of the bath spectral density, $J_k(\omega)$, as

$$C_k(t) = \int_0^\infty d\omega \frac{J_k(\omega)}{\pi} \left[\coth \left(\frac{\beta_k \hbar \omega}{2} \right) \cos(\omega t) - i \sin(\omega t) \right], \quad (2)$$

where $J_k(\omega) \equiv \pi \sum_j g_{k,j}^2 \delta(\omega - \omega_{k,j})$, and β_k is the inverse temperature of the k th bath. The real part of Eq.(2) is analogous to the classical correlation function of the bath and corresponds to the fluctuations, while the imaginary part of its corresponds to the dissipation. The fluctuation term is related to the dissipation term through the quantum version of the FDT.

Here, in order to illustrate the origin of the positivity problem in the Markovian master equation and RE [28, 30], we present the profiles of fluctuation term, $\text{Re}[C(t)]$, for the Drude spectrum, $J(\omega) = \zeta \gamma^2 \omega / (\omega^2 + \gamma^2)$ with ζ and γ being the coupling strength and cutoff frequency, respectively, which will be employed in the subsequent numerical calculations. As shown in Fig. 1, the fluctuation term becomes

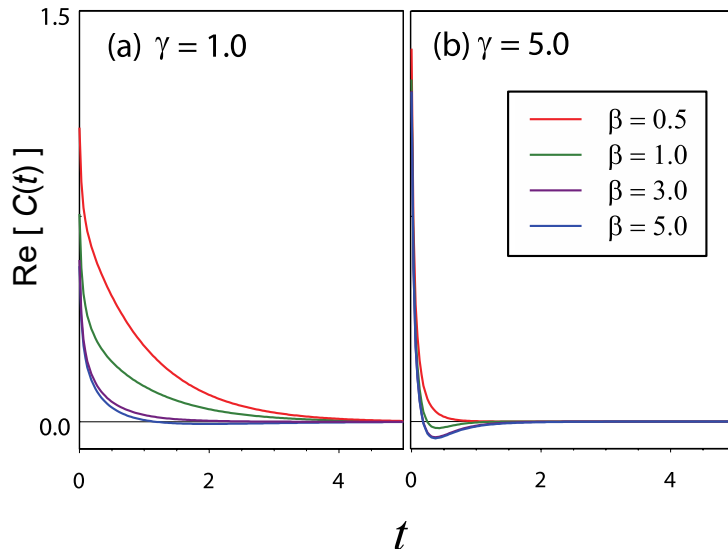


FIG. 1. The real part of Eq.(2), depicted as a function of the dimensionless time t for the intermediate and large values of the inverse noise correlation time: (a) $\gamma = 1$ and (b) $\gamma = 5$ for the Drude spectrum, $J(\omega) = \zeta\gamma^2\omega/(\omega^2 + \gamma^2)$ with $\zeta = 1$. Note that $\gamma \rightarrow \infty$ corresponds to the Markovian (Ohmic) limit. The inverse temperatures are, from top to bottom, $\beta\hbar = 0.5, 1.0, 3.0,$ and 5 . The bath correlation function becomes negative in (a) and (b) at low temperature [28, 30].

negative at low temperature in the region of small t . This behavior is characteristic of quantum noise [28, 30]. We note that the characteristic time scale that we observe $\text{Re}[C(t)] < 0$ is not determined from the bath spectral density $J(\omega)$, but from the bath temperature. Thus, the validity of the Markovian (or $\delta(t)$ -correlated) noise assumption is limited in the quantum case to the high temperature regime. Approaches employing the Markovian master equation and the RE, which are usually applied to systems possessing discretized energy states, ignore or simplify such non-Markovian contributions of the fluctuation, and this is the reason that the positivity condition of the population states is broken. As a method to resolve this problem, the RWA is often employed, but a system treated under this approximation will not satisfy the FDT, and thus the use of such an approximation may introduce significant error in the thermal equilibrium state and in the time evolution of the system toward equilibrium. Because the origin of the positivity problem lies in the unphysical Markovian assumption for the fluctuation term, the situation is better in the non-Markovian case, even within the framework of the RE without the RWA [30].

With the factorized initial conditions we can obtain the exact expression for $\hat{\rho}(t)$, for example, by using the cumulant expansion technique. In the following, the interaction representation of any operator, \hat{A} , with respect to the non-interacting Hamiltonian is expressed as $\hat{A}(t)$. Then, the reduced density operator is written as $\tilde{\rho}(t) = \mathcal{T}_+[\mathcal{U}_{\text{IF}}(t, 0)\hat{\rho}(0)]$, where $\mathcal{U}_{\text{IF}}(t, t_0) = \prod_{k=1}^K \exp[\int_{t_0}^t d\tau W_k(\tau, t_0)]$ is the Feynman-Vernon influence functional in operator form, and $\mathcal{T}_+[\dots]$ is the time-ordering operator, where the operators in $[\dots]$ are arranged in a chronological order. The operators of the influence phase are defined by

$$W_k(\tau, t_0) = \int_{t_0}^{\tau} d\tau' \tilde{\Phi}_k(\tau) \left\{ \text{Re}[C_k(\tau - \tau')] \tilde{\Phi}_k(\tau') - \text{Im}[C_k(\tau - \tau')] \tilde{\Psi}_k(\tau') \right\}, \quad (3)$$

where $\hat{\Phi}_k \hat{A} = (i/\hbar)[\hat{V}_k, \hat{A}]$ and $\hat{\Psi}_k \hat{A} = (1/\hbar)\{\hat{V}_k, \hat{A}\}$. This expression for the reduced density operator, however, does not lead to the closed time-evolution equation.

Then, Tanimura and his collaborators developed the hierarchical equations of motion (HEOM) that consist of the set of equations of motion for the auxiliary density operators (ADOs) as the closed time-evolution equations [25–30]. Here, we consider the case that the bath correlation function, Eq. (2), is written as a linear combination of exponential functions, $C_k(t) = \sum_{l=0}^{L_k} c_{k,l} e^{-\gamma_{k,l}|t|}$, which is realized for the Drude, Lorentz [35, 36], and Brownian bath spectral models [37] (and combinations thereof [38, 39]). Note that, using a set of special functions instead of the exponential functions, we can treat a system with a sub-Ohmic spectral distribution at the zero temperature, where the quantum phase transition occurs [40, 41]. We might include a delta function for better description of the bath correlation function for the HEOM formalism, for example, to approximate the contribution from the higher-order Matsubara

frequency terms [27]. The ADOs introduced in the HEOM are defined by

$$\begin{aligned} \hat{\rho}_{\vec{n}}(t) \equiv & \mathcal{T}_+ \left\{ \exp \left[-\frac{i}{\hbar} \int_0^t ds \mathcal{L}(s) \right] \right\} \\ & \times \mathcal{T}_+ \left\{ \prod_{k=1}^K \prod_{l=0}^{L_k} \left[-\int_0^t d\tau e^{-\gamma_{k,l}(t-\tau)} \hat{\Theta}_{k,l}(\tau) \right]^{n_{k,l}} \mathcal{U}_{\text{IF}}(t, 0) \hat{\rho}(0) \right\}. \end{aligned} \quad (4)$$

Here, we have $\hat{\Theta}_{k,l} \equiv \text{Re}(c_{k,l})\hat{\Phi}_k - \text{Im}(c_{k,l})\hat{\Psi}_k$ and $\mathcal{L}(t)\hat{\rho} = [\hat{H}_{\text{sys}}(t), \hat{\rho}]$. Each ADO is specified by the index $\vec{n} = (n_{1,0}, \dots, n_{1,L_1}, n_{2,0}, \dots, n_{K,L_K})$, where each element takes an integer value larger than zero. The ADO for which all elements are zero, $n_{1,0} = n_{1,1} = \dots = n_{K,L_K} = 0$, corresponds to the actual reduced density operator. Taking the time derivative of Eq.(4), the equations of motion for the ADOs are obtained as

$$\begin{aligned} \frac{d}{dt} \hat{\rho}_{\vec{n}}(t) = & - \left[\frac{i}{\hbar} \mathcal{L}(t) + \sum_{k=1}^K \sum_{l=0}^{L_k} n_{k,l} \gamma_{k,l} \right] \hat{\rho}_{\vec{n}}(t) \\ & - \sum_{k=1}^K \hat{\Phi}_k \sum_{l=0}^{L_k} \hat{\rho}_{\vec{n} + \vec{e}_{k,l}}(t) - \sum_{k=1}^K \sum_{l=0}^{L_k} n_{k,l} \hat{\Theta}_{k,l} \hat{\rho}_{\vec{n} - \vec{e}_{k,l}}(t), \end{aligned} \quad (5)$$

where $\vec{e}_{k,l}$ is the unit vector along the $k \times (l+1)$ th direction. The HEOM consist of an infinite number of equations, but they can be truncated at finite order by ignoring all ADOs beyond the value at which $\sum_{k,l} n_{k,l}$ first exceeds some appropriately large value N . In principle, the HEOM provides an asymptotic approach that allows us to calculate various physical quantities with any desired accuracy by adjusting the number of hierarchal elements determined by N ; the error introduced by the truncation is negligibly small in the case that N is sufficiently large. Note that we can also derive the HEOM for the Fermionic baths [42–44]. Therefore, we can extend the present investigations for the heat transport to the electronic heat current problem.

HEAT CURRENTS

For this system-bath Hamiltonian, the heat current (HC) is defined as the rate of decrease of the bath energy, $\dot{Q}_{\text{HC},k}(t) \equiv -d\langle \hat{H}_{\text{bath}}^{(k)}(t) \rangle / dt$. Using the Heisenberg equations, the heat current can be rewritten as (see Appendix A for the derivation)

$$\dot{Q}_{\text{HC},k}(t) = \dot{Q}_{\text{SEC},k}(t) + \frac{d}{dt} \langle \hat{H}_{\text{int}}^{(k)}(t) \rangle + \sum_{k' \neq k} \dot{I}_{k,k'}, \quad (6)$$

where

$$\dot{Q}_{\text{SEC},k}(t) = \frac{i}{\hbar} \left\langle \left[\hat{H}_{\text{int}}^{(k)}(t), \hat{H}_{\text{sys}}(t) \right] \right\rangle \quad (7)$$

and

$$\dot{I}_{k,k'}(t) = \frac{i}{\hbar} \left\langle \left[\hat{H}_{\text{int}}^{(k)}(t), \hat{H}_{\text{int}}^{(k')}(t) \right] \right\rangle. \quad (8)$$

The first term on the right-hand side of Eq.(6), $\dot{Q}_{\text{SEC},k}$, describes the change of the system energy due to the coupling with the k th bath that is defined as the total k th heat current in the conventional QME approaches, which we call it the system energy current (SEC). The second term vanishes under steady-state conditions and in the limit of a weak system-bath coupling. The third term contributes to the HC even under steady-state conditions, while it vanishes in the weak coupling limit. The third term is the main difference with the SEC. This term plays a significant role in the case that the k th and k' th system-bath interactions are non-commuting and each system-bath coupling is strong. We also note that because this third term is of greater than fourth-order in the system-bath interaction, it does not appear in the second-order QME approach. Therefore only non-perturbative approaches that include higher-order QME approaches allow us to reveal the features. Here, we investigate this contribution using the HEOM theory. Hereafter, we refer to this term as the "tri-partite correlations" (TPC) because the statistical correlation among the k th bath, system, and k' th bath is at least necessary for $I_{k,k'}$ to be present. There

are two physical situations that the TPC contributions of Eq.(8) vanishes: One is that each \hat{V}_k acts on a different Hilbert space of the system, which is realized for a mesoscopic heat-transport system, including nanotubes and nanowires. This is because the left and right reservoirs are coupled to the left and right end degrees of freedom of the system. Another is the cases for $\hat{V}_k \propto \hat{V}_{k'}$, which is often assumed for a simple heat transport system. However, for a microscopic system that includes single-molecular junctions and superconducting qubits, the TPC contribution may play a significant role because of the microscopic manipulation of the system-bath interactions for $[\hat{V}_k, \hat{V}_{k'}] \neq 0$.

Note that, although here we focus only on the first moment of the work and the heat, we can investigate the characteristic features of quantum thermodynamics on the basis of the distribution functions of them by using the HEOM [45] and other approaches [23, 46].

The First and Second Laws of Thermodynamics

In this section, we formulate the first and second laws of quantum thermodynamics that are valid for any system-bath coupling strength, as the natural extensions of the classical thermodynamic laws. This is because we are not sure how the quantum thermodynamic effects emerge into the extension of the classical thermodynamic laws, in particular, in the strong coupling regime. Then we restrict our investigation of the second law in the steady state case, because there is an ambiguity of formulating the second law under non-steady case in a strong coupling regime [21].

We can obtain the first law of thermodynamics by summing Eq.(6) over all k :

$$\sum_{k=1}^K \dot{Q}_{\text{HC},k}(t) = \frac{d}{dt} \left\langle \hat{H}_{\text{sys}}(t) + \sum_{k=1}^K \hat{H}_{\text{int}}^{(k)}(t) \right\rangle - \dot{W}(t), \quad (9)$$

where $\dot{W}(t) = \langle (\partial \hat{H}_{\text{sys}}(t) / \partial t) \rangle$ is the power. The quantity, $\hat{H}_{\text{sys}}(t) + \sum_{k=1}^K \hat{H}_{\text{int}}^{(k)}(t)$, is identified as the internal energy, because the contributions of $\hat{I}_{k,k'}$ cancel out.

In a steady state without external driving forces, the second law is expressed as [47, 48]

$$- \sum_{k=1}^K \beta_k \dot{Q}_{\text{HC},k} \geq 0, \quad (10)$$

while with a periodic external driving force, it is given by

$$- \sum_{k=1}^K \beta_k Q_{\text{HC},k}^{\text{cyc}} \geq 0, \quad (11)$$

where $Q_{\text{HC},k}^{\text{cyc}} = \oint_{\text{cyc}} dt \dot{Q}_{\text{HC},k}(t)$ is the heat absorbed or released per cycle. When the system is coupled to the hot ($k = h$) and the cold ($k = c$) baths and is driven by the periodic field, the heat to work conversion efficiency is bounded by the Carnot efficiency, which is derived by the combination of the first and second laws, as

$$\eta \equiv \frac{-W^{\text{cyc}}}{Q_{\text{HC},k}^{\text{cyc}}} \leq 1 - \frac{\beta_h}{\beta_c}. \quad (12)$$

The second law without a driving force can be rewritten in terms of the SEC as

$$- \sum_{k=1}^K \beta_k \dot{Q}_{\text{SEC},k} \geq \sum_{k,k'=1}^K \beta_k \dot{I}_{k,k'}. \quad (13)$$

When the right-hand side of Eq.(13) is negative, the left-hand side can also take negative values. However, this contradicts the Clausius statement of the second law, i.e., that heat never flows spontaneously from a cold body to a hot body. As we show in the following sections, it is necessary to include the TPC terms to have a thermodynamically valid description.

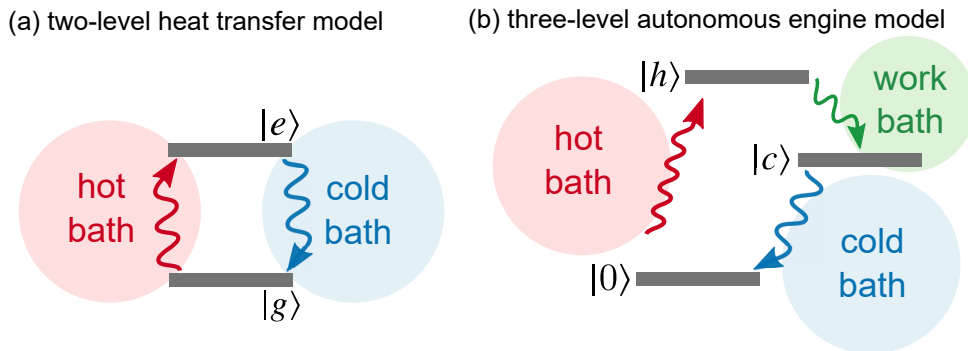


FIG. 2. Schematic depiction of (a) the two-level heat transfer model and (b) the three-level autonomous heat engine model investigated in this study.

REDUCED DESCRIPTION OF HEAT CURRENTS

For the bosonic bath Hamiltonians considered here, we can trace out the bath degrees of freedom in an exact manner by using the second-order cumulant expansion and obtain the reduced expression for the HC, Eq. (6). The derivation is given in Appendix and Ref. [34] in cases that the bath correlation function involves the delta function. The analytical reduced expression for the k th HC is given by

$$\dot{Q}_{\text{HC},k}(t) = \frac{2}{\hbar} \int_0^t d\tau \text{Im} \left[\dot{C}_k(t-\tau) \langle \hat{V}_k(t) \hat{V}_k(\tau) \rangle \right] + \frac{2}{\hbar} \text{Im} [C_k(0)] \langle \hat{V}_k^2(t) \rangle. \quad (14)$$

Note that the second term on the right-hand side of Eq.(14) should vanish as can be seen from the definition of the bath correlation function. However, for the Drude bath spectrum, the contribution of second term is finite, and is found to be necessary to guarantee the first law at least numerically, because of the coarse-grained (long-time approximation) nature of the Drude model [14, 49]. The first term of Eq.(14) consists of non-equilibrium two-time correlation functions of the system operator in the interaction Hamiltonian, and the calculation of these terms seems to be formidable task specifically when the system is driven by the external fields. However, by employing the noise decomposition of the HEOM approach for the bath correlation functions in Eq. (14), and comparing the resulting expressions with the definition of the ADOs given in Eq.(4), we can evaluate the HC in terms of the ADOs as [34]

$$\dot{Q}_{\text{HC},k}(t) = - \sum_{l=0}^{L_k} \gamma_{k,l} \text{Tr} \left[\hat{V}_k \hat{\rho}_{1 \times \vec{e}_{k,l}}(t) \right] + \frac{2}{\hbar} \text{Im} [C_k(0)] \text{Tr} \left[\hat{V}_k^2 \hat{\rho}_0(t) \right]. \quad (15)$$

We note that the ADOs here we employed are the same as that of the conventional HEOM: Using ADOs obtained from the numerical integrating of the HEOM in Eq.(5), we can calculate the HC.

NUMERICAL ILLUSTRATION

To demonstrate a role of the TPC in the HC, we consider a two-level heat transfer model [50–53] and a three-level autonomous heat engine model [18] (Figure 2). We investigate the steady-state HC and SEC obtained from Eq.(5) with the condition $(d/dt)\hat{\rho}_{\vec{n}} = 0$ using the BiCGSafe method for linear equations [54]. We assume that the spectral density of each bath takes the Drude form, $J_k(\omega) = \zeta_k \gamma^2 \omega / (\omega^2 + \gamma^2)$, where ζ_k is the system-bath coupling strength, and γ is the cutoff frequency. A Padé spectral decomposition scheme [55–57] is employed to obtain the expansion coefficients of the bath correlation functions. The accuracy of numerical results is examined by increasing the values of L_1, \dots, L_K and N until convergence is reached.

Two-level heat transfer model

The model studied here consists of a two-level system coupled to two Bosonic baths at different temperatures. This model has been employed extensively as the simplest heat-transport model. The system

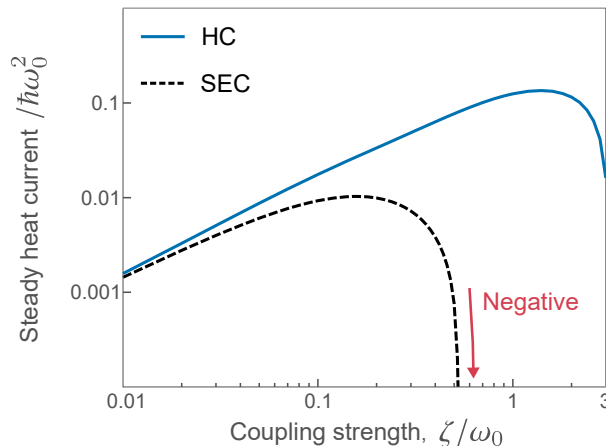


FIG. 3. The heat current (HC) and system energy current (SEC) for the two-level heat transfer model as functions of the system-bath coupling. Both currents are calculated from the HEOM, Eq.(5)

Hamiltonian is given by $\hat{H}_{\text{sys}} = (\hbar\omega_0/2)\sigma_z$. We consider the case in which the system is coupled to the hot bath through $\hat{V}_h = \sigma_x$ and to the cold bath through σ_x and σ_z in the form $\hat{V}_c = (\sigma_x + \sigma_z)/\sqrt{2}$. In order to investigate the difference in the HC with the SEC that usually calculated from the QME approaches, we consider the case $[\hat{V}_h, \hat{V}_c] \neq 0$, because otherwise the TPC term vanishes. This is the case that most of previous investigations have considered. We chose $\beta_h = 0.5 \hbar\omega_0$, $\beta_c = \hbar\omega_0$, and $\gamma = 2\omega_0$.

Figure 3 depicts the HCs in the steady state, $\dot{Q}_{\text{HC},h} = -\dot{Q}_{\text{HC},c}$ or $\dot{Q}_{\text{SEC}} \equiv \dot{Q}_{\text{SEC},h} = -\dot{Q}_{\text{SEC},c}$, as functions of the system-bath coupling strength, $\zeta \equiv \zeta_h = \zeta_c$. In the weak system-bath coupling regime, both HC and SEC increase linearly with the coupling strength in similar manners. In this case, we found that the TPC contribution is minor. As the strength of the system-bath coupling increases, the difference between them becomes large: While \dot{Q}_{SEC} decreases after reaching a maximum value near $\zeta = 0.2\omega_0$, the TPC contribution, $\dot{I}_{h,c}$, dominates the HC, and as a result, it remains relatively large. Thus, in this regime, the SEC becomes much smaller than the HC. In the very strong coupling regime, the SEC eventually becomes negative, which indicates the violation of the second law. In order to eliminate such non-physical behavior, we have to include the $\dot{I}_{h,c}$ term in the definition of the SEC. Note that the differences between the SEC and HC described above vanish when $\hat{V}_c = \hat{V}_h = \sigma_x$, and hence in this case, there is no negative current problem.

Autonomous three-level engine

The autonomous three-level heat engine model considered here consists of three states, denoted by $|0\rangle$, $|h\rangle$, and $|c\rangle$, coupled to three bosonic baths. The work is extracted through the work bath. The system Hamiltonian is expressed as $\hat{H}_{\text{sys}} = \sum_{i=0,h,c} \hbar\omega_i |i\rangle\langle i|$ with $\omega_h > \omega_c > \omega_0$. The system-bath interactions are defined as $\hat{V}_h = |0\rangle\langle h| + |h\rangle\langle 0|$, $\hat{V}_c = |0\rangle\langle c| + |c\rangle\langle 0|$, and $\hat{V}_w = |h\rangle\langle c| + |c\rangle\langle h|$. We set $\omega_0 = 0$ without loss of generality. A mechanism for the system acting as the heat engine is as follows: First, the heat is absorbed from the hot bath. This heat is transferred from the system to the work bath in the form of the work, while the remaining heat is damped into the cold bath. Therefore, the sign conditions for the HC have to be $\dot{Q}_{\text{HC},h} > 0$, $\dot{Q}_{\text{HC},c} < 0$, and $\dot{Q}_{\text{HC},w} < 0$. However, in order to identify the HC to the work bath with the power, the entropy change of the work bath have to be negligibly small, which is realized when the temperature of the work bath becomes infinitely high, $\beta_w \rightarrow 0$ [48, 58, 59]. It should be noted that the stochastic Liouville equation (SLE), in which the back action to the reservoir is ignored, corresponds to the infinite temperature limit of the HEOM [28]. Therefore the entropy calculated from the SLE does not change. When the temperature of the work bath is finite, only the part of the energy extracted from the system can be used as work. However, we show in the following calculation that the system does not act as the engine in the infinitely high temperature limit of the work bath. We set $\omega_c = 0.5\omega_h$, $\zeta_h = \zeta_c = \zeta_w = 0.001\omega_h$, $\gamma = 10\omega_h$, $\beta_h \hbar\omega_h = 0.1$, and $\beta_c \hbar\omega_h = 1$.

In Fig. 4(a), we depict the HC evaluated from the HEOM approach, Eq. (15), SEC, and the HC from the RE approach, as functions of the temperature of the work bath. While the SEC and the HC from the RE approach look identical and weakly dependent on the work-bath temperature with the negative sign,

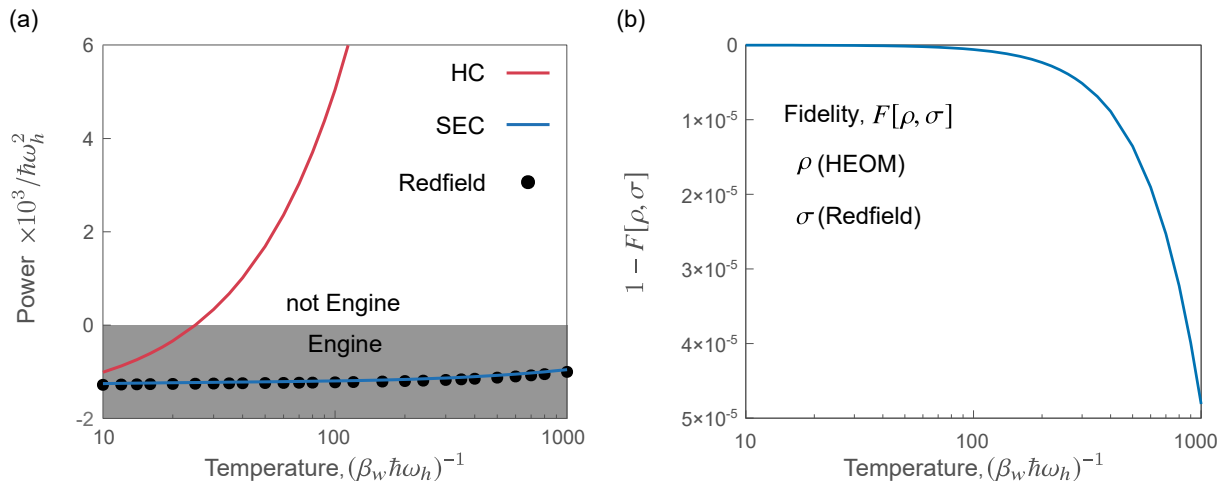


FIG. 4. (a) The heat current (HC, red line) and the system energy current (SEC, blue line) calculated from the HEOM approach, and the HC from the RE approach (black circles) as functions of the temperature of the work bath. The shaded area represents the region that the system acts as the heat engine. (b) The fidelity $F[\rho, \sigma]$ as a function of the temperature of the work bath, where ρ and σ are the reduced density matrix in the steady state calculated from the HEOM and RE approaches, respectively.

the actual HC increases as the temperature of the work bath increases, and eventually its sign changes from negative to positive in the vicinity of $(\beta_w \hbar\omega_h)^{-1} = 20 - 30$. This indicates that the TPC determines the characteristic of the heat-engine system; the system no longer acts as the heat engine.

It should be noted that the TPC effect on the HC becomes important even in the weak system-bath coupling case, as we chose $\zeta = 0.001 \omega_h$. To illustrate this point, we plot the fidelity, $F[\rho, \sigma] = \text{Tr}[\sqrt{\sqrt{\rho}\sigma\sqrt{\rho}}]$, where ρ and σ are the steady state distributions calculated from the HEOM and the RE approaches, respectively, in Fig. 4(b). For all temperature region, the deviation of the fidelity from 1 is negligibly small indicating the system-bath coupling strength is sufficiently weak to be the RE approach valid. This implies that both the HEOM and RE give the identical steady state, while there is large discrepancy between the HEOM and RE results in the calculation of HC in Fig. 4(a). Thus, we have to introduce autonomous heat engine models which are robust against the tri-partite correlations. The theoretical prescription for the finite temperature bath is required to divide the energy obtained from the system into work and heat. Because of the tri-partite correlations, the QME approach is not valid even in the weak-coupling regime.

CONCLUDING REMARKS

In this paper, we introduced an explicit analytical expression for the heat current (HC) on the basis of the energy change of the baths, which includes contributions from the tri-partite correlations (TPC) in addition to that from the system energy current (SEC). Our definition of the HC can be applied to any system with any bath spectral distribution and any strength of the system-bath coupling. Investigation on the basis of the HEOM approach indicated that the HC is physically more appropriate thermodynamics variable than the SEC; the TPC contribution in the heat-engine system is significantly large even in a weak system-bath coupling regime.

In this study, we restricted our analysis to a system described by several energy states. Using the HEOM approach it is possible to investigate a system described by coordinate and momentum (Wigner space) to treat potentials of any form with time-dependent external forces [30, 60]. This feature is ideal for studying quantum transport systems, including the self-current oscillation of a resonant tunneling diode system [61] and the tunneling effect of a ratchet system [62]. Moreover, this treatment allows identification of purely quantum mechanical effects through comparison of classical and quantum results in the Wigner distribution [60, 62, 63].

Although our analysis to this point are limited to the harmonic heat bath, now it becomes possible to study a system with many degrees of freedom, for example, a part of which can be regarded as a spin bath, due to the advent of the computer technology. The numerical implementation of the HEOM by a message passing interface [64], graphical processing unit [65, 66], and the open computer language [67]

or the HEOM combined with the stochastic Schrödinger equation [68–70] are such examples.

We leave such extensions to future studies to be carried out in the context of quantum thermodynamics.

The authors are grateful for motivating us to write this article with Yoshi Oono. A. K. is supported by JSPS KAKENHI Grant Number 17H02946. Y. T. is supported by JSPS KAKENHI Grant Number A26248005.

Appendix A: Derivation of Eq.(6)

The heat current is defined as the rate of decrease of the bath energy, $\dot{Q}_{\text{HC},k}(t) = -d\langle\hat{H}_{\text{bath}}^{(k)}(t)\rangle/dt$, which can be rewritten by using the Heisenberg equations for $\hat{H}_{\text{int}}^{(k)}$ and $\hat{H}_{\text{bath}}^{(k)}$ as

$$\begin{aligned}\dot{Q}_{\text{HC},k}(t) &= \frac{i}{\hbar} \left\langle \left[\hat{H}_{\text{bath}}^{(k)}(t), \hat{H}_{\text{int}}^{(k)}(t) \right] \right\rangle \\ &= \frac{i}{\hbar} \left\langle \left[\hat{H}_{\text{int}}^{(k)}(t), \hat{H}_{\text{sys}}(t) \right] \right\rangle + \frac{d}{dt} \left\langle \hat{H}_{\text{int}}^{(k)}(t) \right\rangle + \sum_{k'} \frac{i}{\hbar} \left\langle \left[\hat{H}_{\text{int}}^{(k)}(t), \hat{H}_{\text{int}}^{(k')}(t) \right] \right\rangle.\end{aligned}\quad (16)$$

The first term of r.h.s. of Eq.(16) is related to the energy flow to the k th bath via the energy conservation equation for \hat{H}_{sys} as $\frac{d}{dt}\langle\hat{H}_{\text{sys}}(t)\rangle = \dot{W}(t) + \sum_k \dot{Q}_{\text{SEC},k}(t)$, where $\dot{Q}_{\text{SEC},k}(t) = (i/\hbar)\langle[\hat{H}_{\text{int}}^{(k)}(t), \hat{H}_{\text{sys}}(t)]\rangle$. Therefore, by using the above definition for $\dot{Q}_{\text{SEC},k}(t)$ and Eq.(8), Eq.(6) is derived.

Appendix B: Derivation of Eq.(14)

To derive Eq.(14), we adapt a generating functional approach by adding the source term, $f_k(t)$, for the k th interaction Hamiltonian as

$$\hat{V}_k \hat{X}_k \rightarrow \hat{V}_{k,f}(t) \hat{X}_k \equiv \left(\hat{V}_k + f_k(t) \right) \hat{X}_k \quad (17)$$

Here, in order to evaluate an expectation value, we add the source term to the ket (left) side of the density operator, which does not change a role of the system-bath interaction in the time-evolution operator. This source term enables us to have a collective bath coordinate with the functional derivative as

$$\tilde{X}_k(t) \tilde{\rho}_{\text{tot}}(t) = i\hbar \frac{\delta}{\delta f_k(t)} \tilde{\rho}_{\text{tot},f}(t) \Big|_{f=0}. \quad (18)$$

Then, the expectation value of the operator $\hat{Z}_k \equiv \hat{A} \hat{X}_k$ for any system operator \hat{A} reads

$$\begin{aligned}\langle \hat{Z}_k(t) \rangle &= \text{Tr}_{\text{sys}} \left[\hat{A}(t) i\hbar \frac{\delta}{\delta f_k(t)} \tilde{\rho}_f(t) \Big|_{f=0} \right] \\ &= \frac{2}{\hbar} \int_0^t d\tau \text{Im} \left[C_k(t-\tau) \langle \hat{A}(t) \hat{V}_k(\tau) \rangle \right].\end{aligned}\quad (19)$$

Next, the k th HC, Eq.(6), is rewritten by using the Heisenberg equation for \hat{V}_k as $\dot{Q}_k(t) = \frac{d}{dt}\langle\hat{H}_{\text{int}}^{(k)}(t)\rangle - \langle(\frac{d}{dt}\hat{V}_k(t))\hat{X}_k(t)\rangle$. The time derivatives, $\frac{d}{dt}\langle\hat{H}_{\text{int}}^{(k)}(t)\rangle$ and $\langle(\frac{d}{dt}\hat{V}_k(t))\hat{X}_k(t)\rangle$, are given by the time differentiation of Eq.(19) for $\hat{A} = \hat{V}_k$ and Eq.(19) for $\hat{A} = \frac{d}{dt}\hat{V}_k$, respectively. This immediately leads to the expression for the k th HC in Eq.(14).

* kato@ims.ac.jp

† tanimura.yoshitaka.5w@kyoto-u.ac.jp

- [1] M. Campisi, P. Hänggi, and P. Talkner, *Rev. Mod. Phys.* **83**, 771 (2011).
- [2] A. Polkovnikov, K. Sengupta, A. Silva, and M. Vengalattore, *Rev. Mod. Phys.* **83**, 863 (2011).
- [3] J. Eisert, M. Friesdorf, and C. Gogolin, *Nat. Phys.* **11**, 124 (2015).
- [4] M. Lostaglio, K. Korzekwa, D. Jennings, and T. Rudolph, *Phys. Rev. X* **5**, 021001 (2015).
- [5] K. Korzekwa, M. Lostaglio, J. Oppenheim, and D. Jennings, *New J. Phys.* **18**, 023045 (2016).

- [6] H. P. Breuer and F. Petruccione, *The Theory of Open Quantum Systems* (Oxford University Press, New York, 2002).
- [7] R. Kosloff, *Entropy* **15**, 2100 (2013).
- [8] P. Haggi and G.-L. Ingold, *Chaos* **15**, 026105 (2005).
- [9] T. Harada and S. Sasa, *Phys. Rev. Lett.* **95**, 130602 (2005).
- [10] K. Saito, *Europhys. Lett.* **83**, 50006 (2008).
- [11] P. Hofer, M. Perarnau-Llobet, L. Miranda, M. David, G. Haack, R. Silva, J. B. Brask, and N. Brunner, *New J. Phys.* **19**, 123037 (2017).
- [12] J. O. Gonzalez, L. A. Correa, G. Nocerino, J. P. Palao, D. Alonso, and G. Adesso, *Open Syst. Inf. Dyn.* **24**, 1740010 (2017).
- [13] M. T. Mitchison and M. B. Plenio, *New J. Phys.* **20**, 033005 (2018).
- [14] A. Ishizaki and G. Fleming, *J. Chem. Phys.* **130**, 234111 (2009).
- [15] S. Huelga and M. Plenio, *Contemp. Phys.* **54**, 181 (2013).
- [16] I. de Vega and D. Alonso, *Rev. Mod. Phys.* **89**, 015001 (2017).
- [17] D. Gelbwaser-Klimovsky and A. Aspuru-Guzik, *J. Phys. Chem. Lett.* **6**, 3477 (2015).
- [18] P. Strasberg, G. Schaller, N. Lambert, and T. Brandes, *New J. Phys.* **18**, 073007 (2016).
- [19] D. Newman, F. Mintert, and A. Nazir, *Phys. Rev. E* **95**, 032139 (2017).
- [20] M. Esposito, M. A. Ochoa, and M. Galperin, *Phys. Rev. Lett.* **114**, 080602 (2015).
- [21] M. Esposito, M. A. Ochoa, and M. Galperin, *Phys. Rev. B* **92**, 235440 (2015).
- [22] A. Bruch, M. Thomas, S. V. Kusminskiy, F. von Oppen, and A. Nitzan, *Phys. Rev. B* **93**, 115318 (2016).
- [23] M. Carrega, P. Solinas, M. Sasseti, and U. Weiss, *Phys. Rev. Lett.* **116**, 240403 (2016).
- [24] R. Schmidt, M. F. Carusela, J. P. Pekola, S. Suomela, and J. Ankerhold, *Phys. Rev. B* **91**, 224303 (2015).
- [25] Y. Tanimura and R. Kubo, *J. Phys. Soc. Jpn.* **58**, 101 (1989).
- [26] Y. Tanimura, *Phys. Rev. A* **41**, 6676 (1990).
- [27] A. Ishizaki and Y. Tanimura, *J. Phys. Soc. Jpn.* **74**, 3131 (2005).
- [28] Y. Tanimura, *J. Phys. Soc. Jpn.* **75**, 082001 (2006).
- [29] Y. Tanimura, *J. Chem. Phys.* **141**, 044114 (2014).
- [30] Y. Tanimura, *J. Chem. Phys.* **142**, 144110 (2015).
- [31] A. G. Dijkstra and Y. Tanimura, *Phys. Rev. Lett.* **104**, 250401 (2010).
- [32] A. G. Dijkstra and Y. Tanimura, *J. Phys. Soc. Jpn.* **81**, 063301 (2012).
- [33] A. Kato and Y. Tanimura, *J. Chem. Phys.* **143**, 064107 (2015).
- [34] A. Kato and Y. Tanimura, *J. Chem. Phys.* **145**, 224105 (2016).
- [35] C. Kreisbeck and T. Kramer, *J. Phys. Chem. Lett.* **3**, 2828 (2012).
- [36] J. Ma, Z. Sun, X. Wang, and F. Nori, *Phys. Rev. A* **85**, 062323 (2012).
- [37] M. Tanaka and Y. Tanimura, *J. Phys. Soc. Jpn.* **78**, 073802 (2009).
- [38] H. Liu, L. Zhu, S. Bai, and Q. Shi, *J. Chem. Phys.* **140**, 134106 (2014).
- [39] Y. Tanimura, *J. Chem. Phys.* **137**, 22A550 (2012).
- [40] Z. Tang, O. Z. Gong, H. Wang, J. Wu, *J. Chem. Phys.* **143**, 224112 (2015).
- [41] C. Duan, Z. Tang, J. Cao, and J. Wu, *Phys. Rev. B* **95**, 214308 (2017).
- [42] J. Jin, X. Zheng, and Y. Yan, *J. Chem. Phys.* **128**, 234703 (2008).
- [43] R. Hartle, G. Cohen, D. R. Reichman, and A. J. Millis, *Phys. Rev. B* **88**, 235426 (2013).
- [44] L. Ye, X. Wang, D. Hou, R.-X. Xu, X. Zheng, and Y. Yan, *WIREs Comput. Mol. Sci.* **6**, 608 (2016).
- [45] J. Cerrillo, M. Buser, and T. Brandes, *Phys. Rev. B* **94**, 214308 (2016).
- [46] E. Aurell, *arXiv:1801.04235*.
- [47] S. Deffner and C. Jarzynski, *Phys. Rev. X* **3**, 041003 (2013).
- [48] P. Strasberg, G. Schaller, T. Brandes, and M. Esposito, *Phys. Rev. X* **7**, 021003 (2017).
- [49] R. Kubo, M. Toda, and N. Hashitsume, *Statistical Physics II: Nonequilibrium Statistical Mechanics* (Springer-Verlag, Berlin, 1985).
- [50] D. Segal and A. Nitzan, *Phys. Rev. Lett.* **94**, 034301 (2005).
- [51] K. A. Velizhanin, H. Wang, and M. Thoss, *Chem. Phys. Lett.* **460**, 325 (2008).
- [52] T. Ruokola and T. Ojanen, *Phys. Rev. B* **83**, 045417 (2011).
- [53] C. Wang, J. Ren, and J. Cao, *Sci. Rep.* **5**, 11787 (2015).
- [54] S. Fujino, M. Fujiwara, and M. Yoshida, *Transactions of JSCES* **8**, 145 (2005) [in Japanese].
- [55] J. Hu, R. X. Xu, Y. J. Yan, *J. Chem. Phys.* **133**, 101106 (2010).
- [56] B. L. Tian, J. J. Ding, R. X. Xu, Y. J. Yan, *J. Chem. Phys.* **133**, 114112 (2010).
- [57] J. Hu, M. Luo, F. Jiang, R.-X. Xu, and Y. Yan, *J. Chem. Phys.* **134**, 244106 (2011).
- [58] J. E. Geusic, E. O. Schulz-DuBios, and H. E. D. Scovil, *Phys. Rev.* **156**, 343 (1967).
- [59] M. P. Woods, N. Ng, and S. Wehner, *arXiv: 1506.02322*.
- [60] Y. Tanimura and P. G. Wolynes, *J. Chem. Phys.* **96**, 8485 (1992).
- [61] A. Sakurai and Y. Tanimura, *New J. Phys.* **16**, 015002 (2014).
- [62] A. Kato and Y. Tanimura, *J. Phys. Chem. B* **117**, 13132 (2013).
- [63] A. Sakurai and Y. Tanimura, *J. Phys. Chem. A* **115**, 4009 (2011).
- [64] J. Strumpfer and K. Schulten, *J. Chem. Theory Comput.* **8**, 2808 (2012).
- [65] M. Tsuchimoto and Y. Tanimura, *J. Chem. Theory Comput.* **11**, 3859 (2015).
- [66] C. Kreisbeck, T. Kramer, M. Rodriguez, and B. Hein, *J. Chem. Theory Comput.* **7**, 2166 (2011).
- [67] C. Kreisbeck, T. Kramer, and A. Aspuru-Guzik, *J. Chem. Theory Comput.* **10**, 4045 (2014).

- [68] D. Suess, A. Eisfeld, and W. T. Strunz, *Phys. Rev. Lett.* **113**, 150403 (2014).
- [69] K. Song, L. Song, and Q. Shi, *J. Chem. Phys.* **144**, 224105 (2016).
- [70] Y. Ke and Y. Zhao, *J. Chem. Phys.* **145**, 024101 (2016).